nature geoscience

SUPPLEMENTARY INFORMATION

DOI: 10.1038/NGEO2630

# Amplification of El Niño by cloud longwave coupling to atmospheric circulation

Gaby Rädel, Thorsten Mauritsen, Bjorn Stevens, Dietmar Dommenget, Daniela Matei, Katinka Bellomo and Amy Clement

DOI: 10.1038/NGEO2630

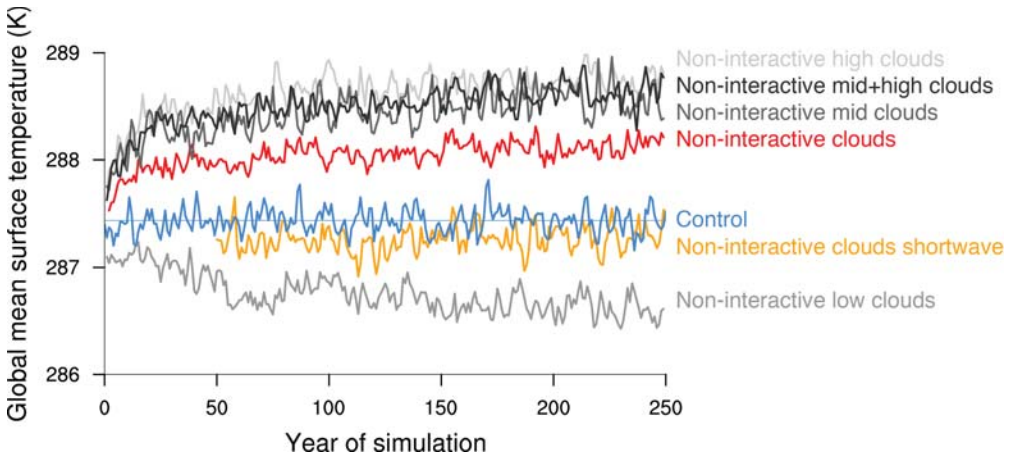


Figure S1: Global mean temperature in experiments. Thin blue line is the time mean of the full 1000-year control simulation. In the experiment with non-interactive clouds in shortwave only (orange) the data from the first 50 years have not been retained.

Table S1: Surface temperature variance in observations and in experiments with MPI-ESM-LR for various standard Nino regions. Units are $K^2$.

| | Nino-4 | Nino-3.4 | Nino-3 | Nino-1+2 |
|---|---|---|---|---|
| Observed (HadISST) | 0.31 | 0.58 | 0.61 | 0.80 |
| Control | 0.49 | 0.57 | 0.59 | 0.69 |
| Non-interactive clouds (realisation 1) | 0.18 | 0.20 | 0.24 | 0.46 |
| Non-interactive clouds (realisation 2) | 0.21 | 0.21 | 0.26 | 0.46 |
| Non-interactive clouds in shortwave | 0.57 | 0.63 | 0.60 | 0.66 |
| Non-interactive low-level clouds | 0.24 | 0.25 | 0.46 | 0.47 |
| Non-interactive mid-level clouds | 0.79 | 0.95 | 0.92 | 0.92 |
| Non-interactive high-level clouds | 0.34 | 0.38 | 0.46 | 0.73 |
| Non-interactive mid+high-level clouds | 0.46 | 0.52 | 0.60 | 0.80 |

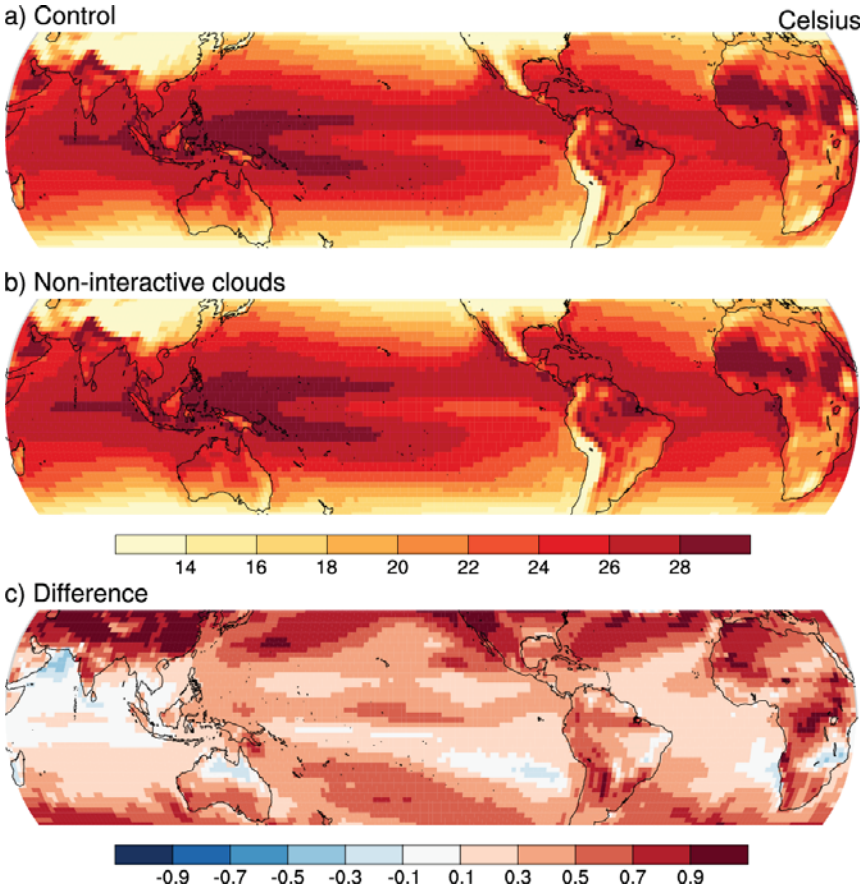


Figure S2: Surface temperature in the control and non-interactive cloud experiments and their difference.

DOI: 10.1038/NGEO2630

Table S2: Standard dynamical Bjerknes feedback between SST in the Nino-3 region and zonal surface windstress in the Nino-4 region, and surface heat flux feedback (Nino-3) for the experiments with MPI-ESM-LR.

| | Bjerknes feedback ($\mu$) ($10^{-3}$Nm$^{-2}$K$^{-1}$) | Surface flux feedback ($\alpha$) (Wm$^{-2}$K$^{-1}$) |
|---|---|---|
| Control | 3.9 | -3.5 |
| Non-interactive clouds (realisation 1) | 3.0 | -6.2 |
| Non-interactive clouds (realisation 2) | 3.0 | -6.0 |
| Non-interactive clouds in shortwave | 4.3 | n/a |
| Non-interactive low-level clouds | 3.5 | -6.9 |
| Non-interactive mid-level clouds | 4.6 | -4.3 |
| Non-interactive high-level clouds | 3.5 | -3.7 |
| Non-interactive mid+high-level clouds | 3.2 | -3.5 |

Table S3: Standard errors derived from 100-member historical (1850-2005) ensemble of MPI-ESM1.1-LR. Columns with numbers of years are calculated from the ensemble standard error as described in methods.

| | Ensemble | 27 years | 200 years | 1000 years |
|---|---|---|---|---|
| Nino-4 standard deviation (K) | 0.05 | 0.12 | 0.05 | 0.02 |
| Nino-3.4 standard deviation (K) | 0.06 | 0.14 | 0.05 | 0.02 |
| Nino-3 standard deviation (K) | 0.05 | 0.11 | 0.04 | 0.02 |
| Nino-4 variance (K$^2$) | 0.09 | 0.20 | 0.08 | 0.03 |
| Nino-3.4 variance (K$^2$) | 0.09 | 0.22 | 0.08 | 0.04 |
| Nino-3 variance (K$^2$) | 0.07 | 0.18 | 0.06 | 0.03 |
| Bjerknes feedback ($\mu$) ($10^{-3}$Nm$^{-2}$K$^{-1}$) | 0.4 | 1.0 | 0.4 | 0.2 |
| Surface flux feedback ($\alpha$) (Wm$^{-2}$K$^{-1}$) | 0.3 | 0.7 | 0.3 | 0.1 |
| Nino-4 TOA longwave feedback (Wm$^{-2}$K$^{-1}$) | 0.6 | 1.4 | 0.5 | 0.2 |

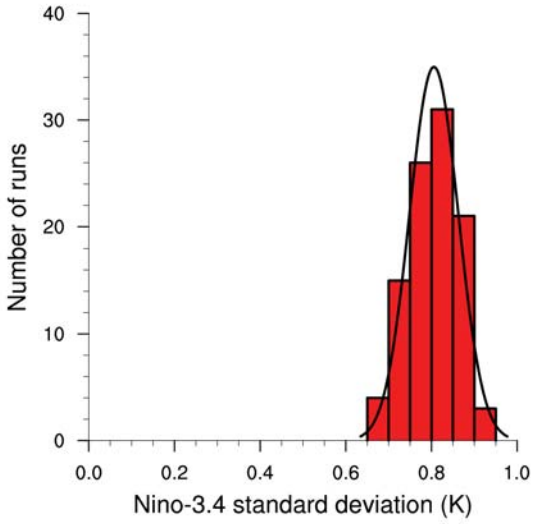


Figure S3: Distribution (red) of Nino-3.4 standard deviation in the 100-member ensemble of historical simulations (1850-2005) with MPI-ESM1.1-LR. Also shown is a fitted normal distribution (black line).

DOI: 10.1038/NGEO2630

Table S4: Overview of CMIP5 runs used in Figure 4. The units of Nino-3.4 temperature standard deviation ($\sigma_{T_{3.4}}$) is K and of maximum longwave feedback regressed on Nino-3.4 temperature ($\mathrm{LW_{Max}}$) it is $\mathrm{Wm^{-2}K^{-1}}$.

| Model Name | $\sigma_{T_{3.4}}$ | $\mathrm{LW_{Max}}$ | Years | Reference |
|---|---|---|---|---|
| ACCESS1-0 | 0.65 | 26.12 | 500 | [33] |
| ACCESS1-3 | 0.66 | 21.20 | 500 | ” |
| BCC-CSM1-1 | 0.70 | 12.41 | 500 | [34] |
| BCC-CSM1-1-M | 1.32 | 14.40 | 400 | ” |
| BNU-ESM | 1.23 | 16.76 | 559 | [35] |
| CanESM2 | 0.84 | 25.67 | 996 | [36] |
| CCSM4 | 0.89 | 20.37 | 501 | [37] |
| CESM1-CAM5 | 0.82 | 21.37 | 319 | [38] |
| CESM1-BGC | 0.88 | 20.92 | 500 | ” |
| CESM1-WACCM | 1.15 | 17.93 | 200 | ” |
| CESM1-FastChem | 0.84 | 21.11 | 222 | ” |
| CMCC-CESM | 1.62 | 13.38 | 277 | n/a |
| CMCC-CMS | 0.80 | 28.30 | 500 | ” |
| CMCC-CM | 0.57 | 31.66 | 330 | ” |
| CNRM-CM5 | 0.82 | 18.47 | 850 | [39] |
| CSIRO-Mk3-6-0 | 0.68 | 12.88 | 500 | [40] |
| FGOALS-g2 | 0.75 | 15.19 | 300 | [41] |
| GFDL-CM3 | 0.93 | 29.8 | 500 | [42] |
| GFDL-ESM2G | 0.72 | 24.02 | 500 | [43] |
| GFDL-ESM2M | 1.18 | 20.08 | 500 | ” |
| GISS-E2-H-CC | 0.75 | 13.91 | 251 | [44] |
| GISS-E2-R | 0.50 | 18.74 | 850 | ” |
| GISS-E2-R-CC | 0.50 | 18.83 | 251 | ” |
| HadGEM2-ES | 0.73 | 19.50 | 577 | [45] |
| INMCM4 | 0.41 | 10.50 | 500 | [46] |
| IPSL-CM5A-LR | 0.64 | 18.98 | 1000 | [47] |
| IPSL-CM5A-MR | 0.75 | 15.91 | 300 | ” |
| IPSL-CM5B-LR | 0.61 | 38.94 | 300 | [48] |
| MIROC5 | 0.76 | 19.48 | 670 | [49] |
| MIROC-ESM-CHEM | 0.44 | 12.89 | 225 | [50] |
| MIROC-ESM | 0.43 | 11.73 | 630 | ” |
| MPI-ESM-LR | 0.77 | 15.25 | 1000 | [22, 51] |
| MPI-ESM-MR | 0.68 | 15.44 | 1000 | ” |
| MPI-ESM-P | 0.77 | 15.67 | 1156 | ” |
| MRI-CGCM3 | 0.63 | 20.25 | 500 | [52] |
| MRI-AGCM3-2H | 0.77 | 15.67 | 1156 | ” |
| NorESM1-M | 0.66 | 28.59 | 501 | [53] |

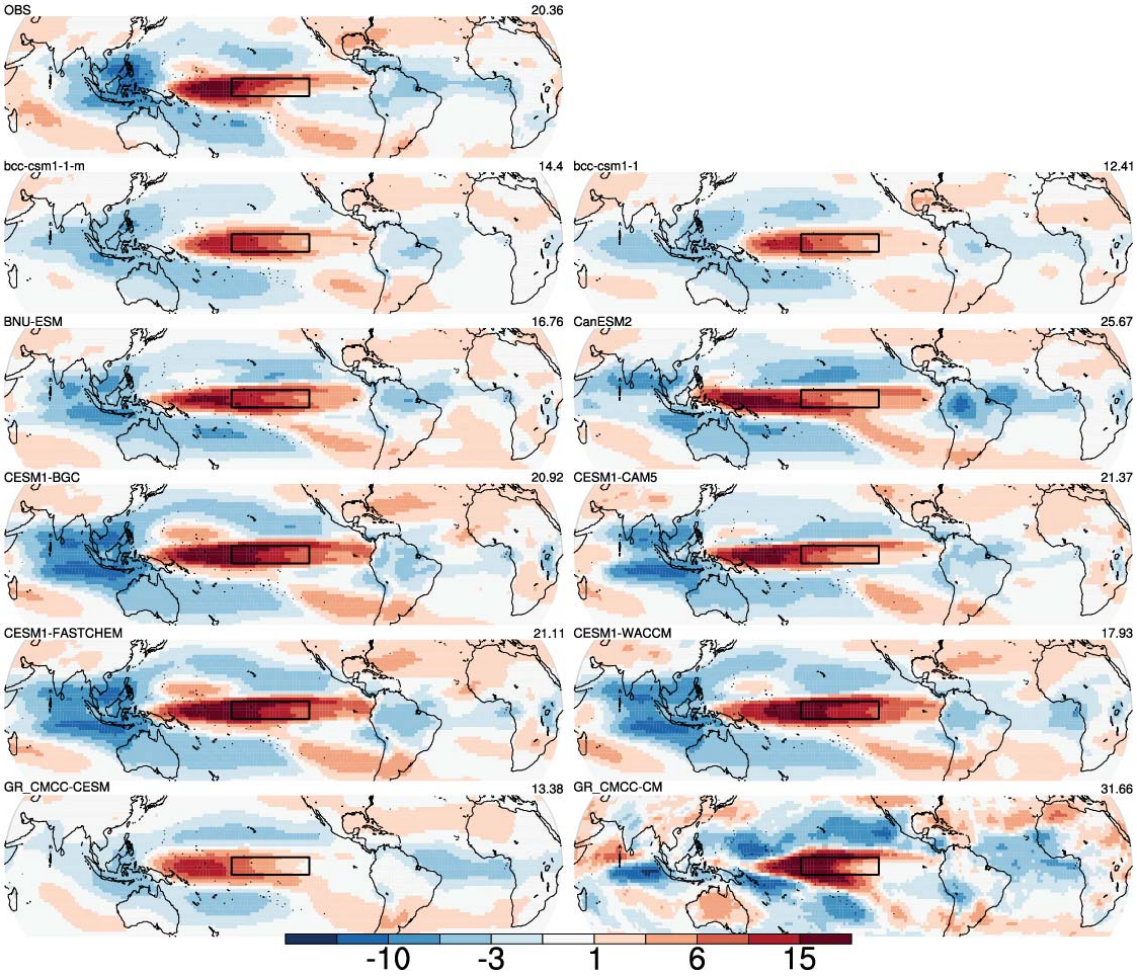


Figure S4: Regression of top-of-atmosphere net longwave irradiance for observations and individual CMIP5 models listed in Table S4.

DOI: 10.1038/NGEO2630

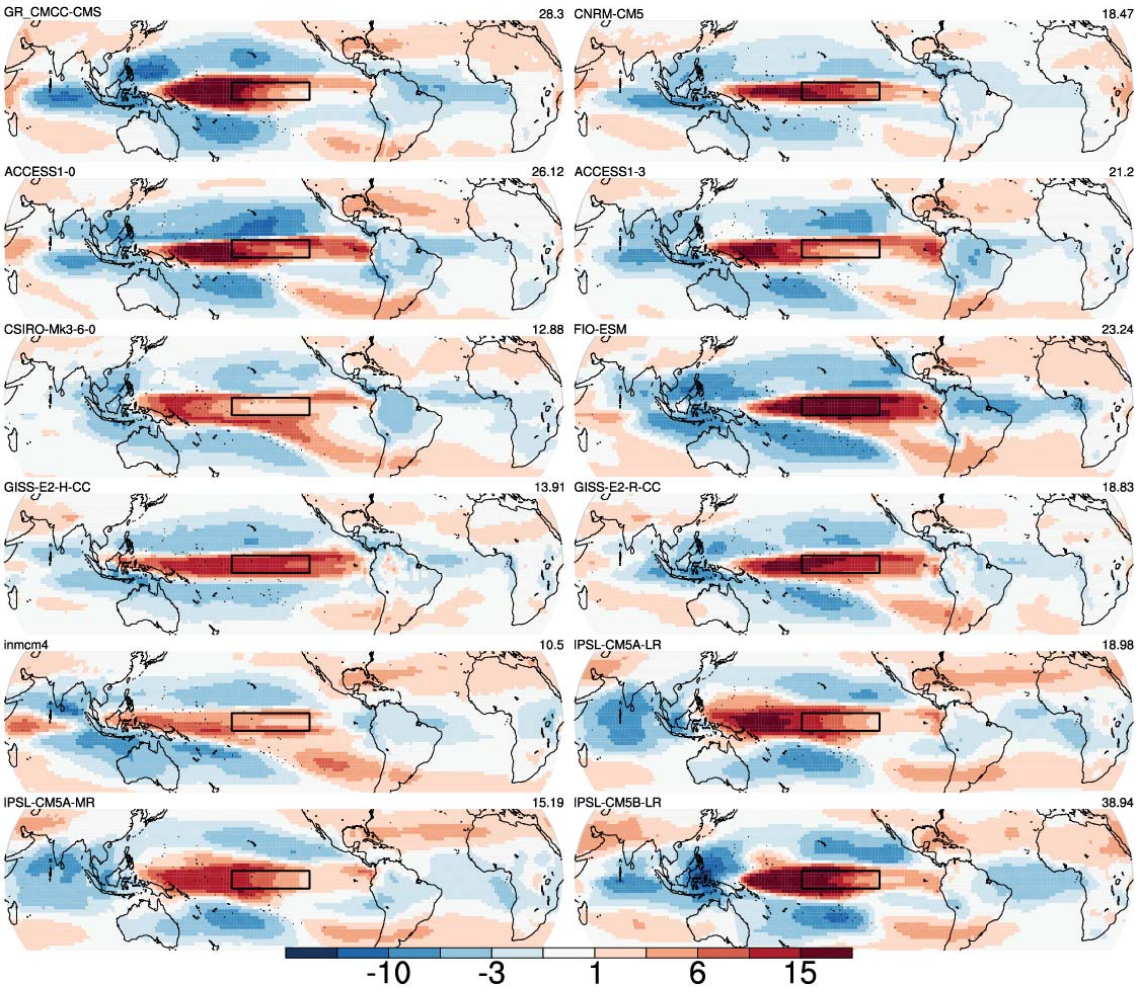


Figure S5: Continued from Figure S4.

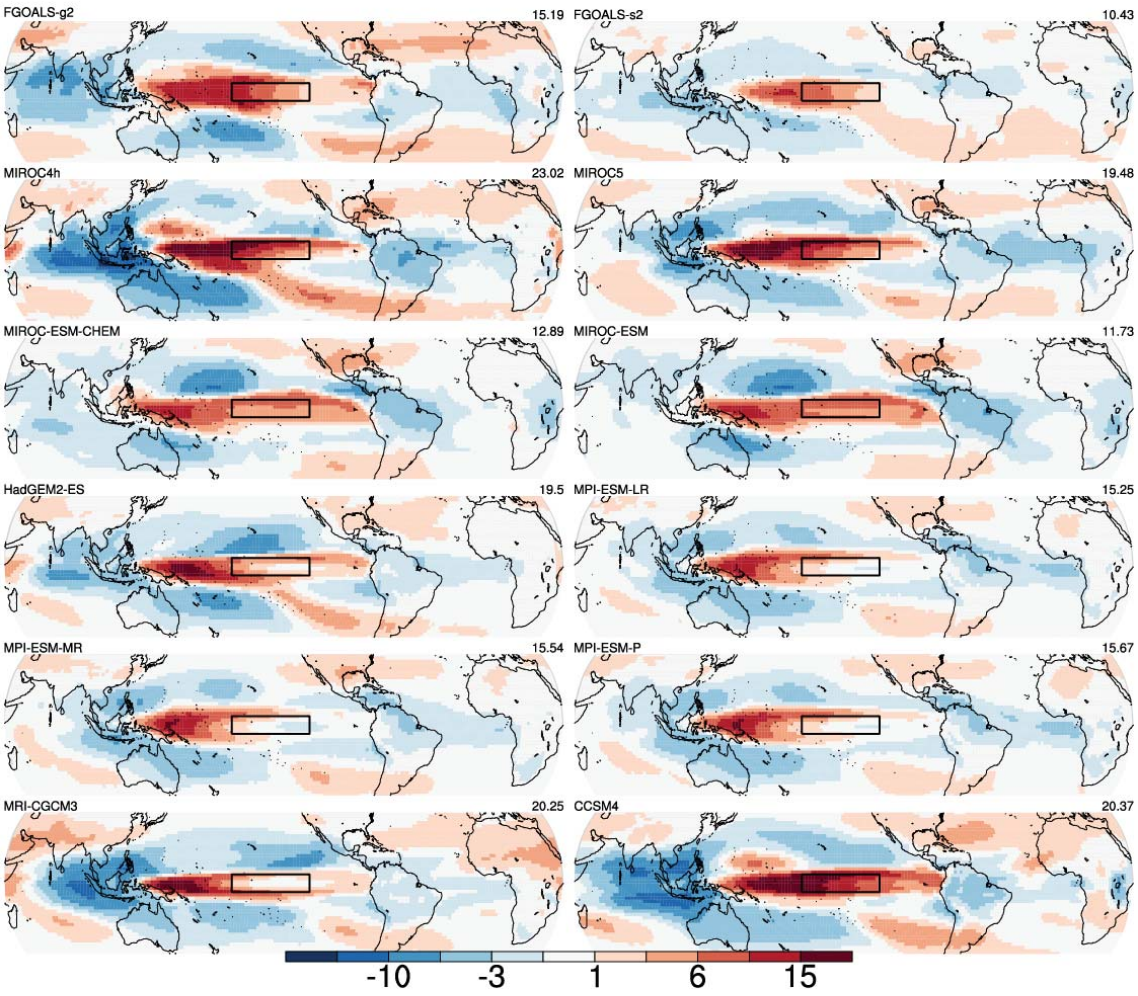


Figure S6: Continued from Figure S5.

DOI: 10.1038/NGEO2630

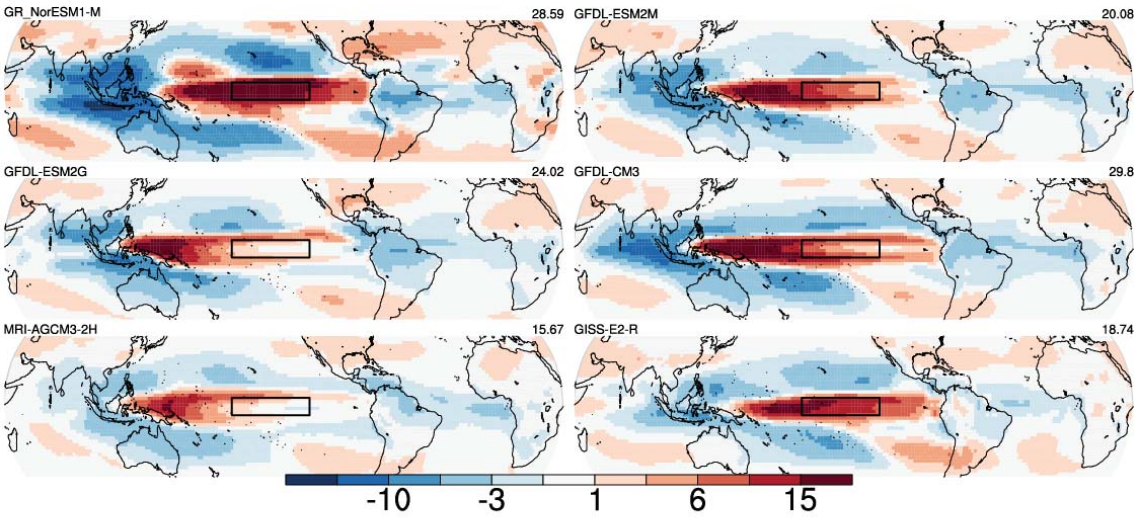


Figure S7: Continued from Figure S6.